Tight-binding calculations of quasiparticle wave functions for C(111)2×1

Margherita Marsili,[1,2] Olivia Pulci,[1,2] Friedhelm Bechstedt,[1,3] and Rodolfo Del Sole[1,2]
[1]*European Theoretical Spectroscopy Facility (ETSF)*
[2]*CNR-INFM-SMC NAST, Dipartimento di Fisica, Università di "Tor Vergata," Via della Ricerca Scientifica 1, 00133 Roma, Italy*
[3]*IFTO, Friedrich Schiller Universität, Max-Wien-Platz 1, D-07743 Jena, Germany*
(Received 2 July 2008; published 10 November 2008)

Despite the simplicity of the system, the description of the excited-state properties of the cleavage surface of diamond requires the use of nonstandard treatment of many-body effects. Using a simple tight-binding model, we show that the typical assumption concerning the identity of quasiparticle and Kohn-Sham wave functions fails in an important part of the Brillouin zone. This simple model allows computation of the qualitatively different quasiparticle wave functions. The optical properties calculated with these wave functions at the Bethe-Salpeter level show important excitonic effects. Moreover the line shape of the reflectance anisotropy spectrum is significantly improved when compared to the measured one.

DOI: 10.1103/PhysRevB.78.205414 PACS number(s): 73.20.At, 71.10.−w

I. INTRODUCTION

Chemical vapor deposition (CVD) techniques, permitting the low cost fabrication of high quality diamond,[1] have brought up considerable interest in diamond, especially for the exploitation of its extreme electronic and chemical properties in (bio)technological devices.[2] Its great surface chemical inertness and high degree of biocompatibility make diamond well suited for biomedical applications. Moreover the increasing crystal quality of phosphorus and boron-doped homoepitaxial diamond films[3] opens the way for manufacturing high quality electronic devices.

The surface properties of diamond are in part similar to Ge and Si surface properties. However there are some important differences: starting from the details of the reconstructions and going on to the negative electron affinity of the hydrogen-terminated diamond surfaces to the possibility of surface transfer doping.[4]

In this work we focus our attention to the clean, reconstructed (111) surface of diamond. The (111) plane is the cleavage face of diamond and one of the growth planes during the CVD process. With respect to C(100), which is the other CVD growth plane, C(111) shows a higher electron mobility in phosphorus-doped samples,[3] a higher boron incorporation rate,[5] and a higher transition temperature of superconducting boron-doped diamond.[6] All these properties, together with the improved crystalline quality recently achieved,[3] make this surface technologically relevant. The clean (111) 2×1 reconstructed surface is in principle a simple prototypical system; however important issues concerning its electronic and optical properties are not fully understood.

Right after cleavage the (111) surface of diamond is unreconstructed with each dangling bond saturated by a hydrogen atom. After annealing at more than 700 K, hydrogen desorbs and the surface shows a 2×1 reconstruction. The reconstruction geometry, shown in Fig. 1(a), involves a strong rearrangement of the top layer atoms, forming the so-called π-bonded Pandey chains[7] along the y direction. Contrary to the case of the cleavage surface of Si and Ge, the atoms belonging to the chains are neither buckled nor dimerized in all well converged ground-state calculations.[8] The dispersion of the electronic surface bands can bear witness to the presence of one-dimensional structures in the reconstruction. In fact, angle-resolved photoemission spectra (ARPES) show that the occupied surface bands have a strong dispersion along the chain direction [$\Gamma-J$ and $J'-K$ in the irreducible Brillouin zone (IBZ), see Fig. 1(b)] and are almost flat perpendicular to it (i.e., along the $J-K$ and $\Gamma-J'$ directions).[9] Density-functional theory (DFT) (Ref. 10) band-structure calculations[8] are able to well reproduce the occupied surface-state dispersion. However, all the calculations show that the surface is semimetallic, with the surface bands crossing the Fermi level at the $J-K$ line. The existence of a gap in the quasiparticle (QP) band structure of the surface can be found by theory only through the careful treatment of many-body effects by an iterative GW (Ref. 11) procedure.[12] This procedure leads to a minimum direct gap of about 1 eV, in rough agreement with the onset of energy-loss spectra.[13] Even so, recent reflectance anisotropy spectra (RAS) (Ref. 14) revealed a larger optical gap of 1.47 eV.[15]

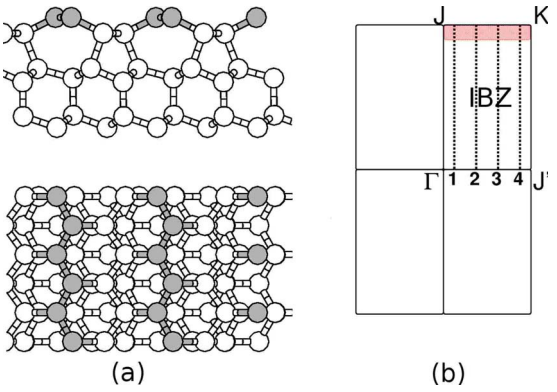

FIG. 1. (Color online) (a) Ground-state geometry of the (111) surface of diamond and (b) its first Brillouin zone. The top panel in (a) is the side view of the first atomic layers while the bottom panel is the top view of the surface. Carbon atoms belonging to the surface π-bonded chains are in gray. The four lines along which the IBZ is sampled are shown in (b). The QP wave functions have been computed for the k points within the red-shaded area.

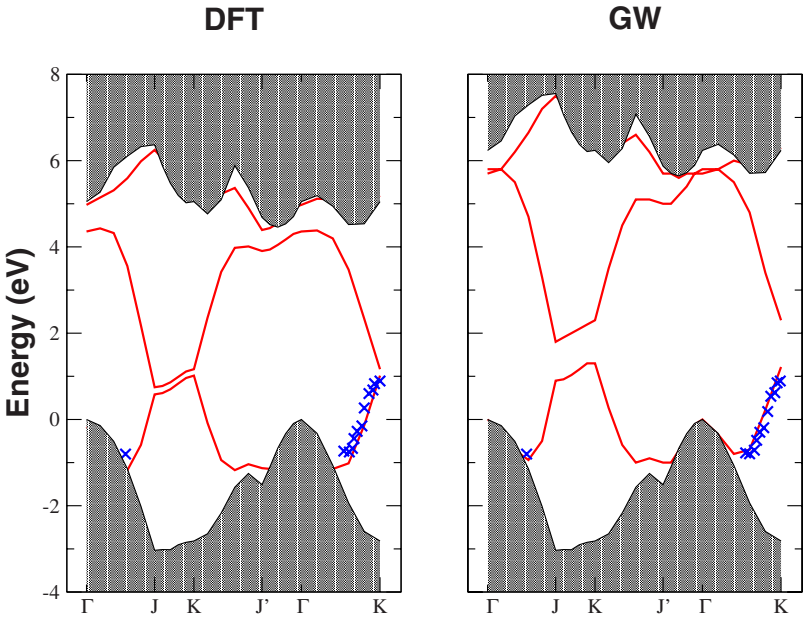

FIG. 2. (Color online) DFT (left) and *GW* (right) band structures from Ref. 12. Crosses: experiments from Refs. 9 and 35.

This result, especially taking into account the possibility of significant excitonic effects,[16] calls for further theoretical investigations to understand and correct the underestimation of the electronic gap.

A larger electronic gap could be obtained if the chains varied from their unbuckled, undimerized geometry.[17,18] However, dimerization is ruled out by experiments.[9] Buckling is not completely ruled out[19,20] but within DFT it appears energetically unfavorable whatever functional is used for the exchange-correlation potential.[21] Moreover, low-energy electron-diffraction (LEED) spot intensity vs voltage data[22] compared to the DFT results show a very good agreement for all the structural parameters.[23]

The state of the art theoretical tool for the determination of the quasiparticle electronic structure of materials is based on the so-called *GW* approximation.[11] This approach, within the framework of many-body perturbation theory, consists in evaluating the electronic self-energy Σ as the product of the Green's function G and the screened Coulomb interaction W, namely $\Sigma(1,2)=iG(1,2)W(2,1)$, where $\{1,2\}$ stand for time, space, and spin indexes. The *GW* approximation neglects the vertex corrections in the expression of self-energy. However, this is not the only approximation that is applied. Usually, the QP band structure is obtained by taking into account self-energy effects in a first-order perturbation scheme with respect to the unperturbed Kohn-Sham (KS) Hamiltonian.[10] Moreover, since the true Green's function and the true screened Coulomb interaction are unknown, the self-energy and its matrix elements, as well as the random-phase approximation (RPA) dielectric matrix, are computed by means of the KS eigenvalues and eigenfunctions of the DFT. This is the so-called G_0W_0 approximation of the self-energy. G_0W_0 has been proven to be a very reliable scheme on a variety of materials.[24] However, as shown in Ref. 12, G_0W_0 fails in reproducing even qualitatively the semiconducting character of C(111)2×1. As mentioned above, the semiconducting character of this surface can be restored through a self-consistent procedure, yielding a minimum direct gap of 1 eV. During each cycle of this procedure, the QP energies are updated in both G and W but *the wave functions are kept fixed* to their original KS values.

In many semiconductors, in fact, KS orbitals describe quite well the corresponding QP wave functions.[11,25,26] Nevertheless, it is sometimes necessary to go beyond this level of approximation. In fact, to correctly describe the single-particle excited states of different systems, it has been essential in some cases to diagonalize the self-energy matrix,[27–29] in some other cases to use wave functions stemming from nonlocal potentials,[30–34] or finally to achieve a full self-consistent solution of the Dyson equation.[25,33] In this paper we want to analyze if, also for C(111), the KS wave functions are unsuited to describe the QP orbitals. The large surface gap corrections (from 0.1 to about 1 eV, see Fig. 2) strongly suggest that the QP wave functions are different from DFT ones. In order to shed light on this point, we modeled the quasiparticle electronic structure of the surface chains within a tight-binding model. We will show that, whereas at the *JK* line the QP wave functions and the DFT ones are the same by symmetry, in a region very close to it, where the DFT gap is much smaller than the *GW* correction, the QP wave functions are very much different from the DFT ones. Our results show that, when exciting the system upon adding an electron or a hole, the probability to find the particle is localized on one of two chain atoms. This excited-state physics apparently cannot be captured by a ground-state theory, such as DFT, where the discrimination of the two atoms can stem only from a geometric distortion that, in the case of diamond, proves to be too expensive from an elastic energy point of view.

The paper is organized as follows: first we introduce the chain model. Then we describe the QP wave function (calculated within tight binding) and compare them to the KS ones. Finally, we will demonstrate how the QP wave functions influence the reflectance anisotropy (RA) spectrum.

II. MODEL QUASIPARTICLE WAVE FUNCTIONS OF SURFACE BANDS

For the C(111)2×1 surface, the two π and π^* related surface bands are well energetically separated from the projected bulk band structure. This fact allows us to use a simple model based on one-dimensional chains with two carbon atoms per unit cell, the lattice parameter being a. Each chain atom has one atomic orbital ϕ_1 or ϕ_2, which represents the surface-atom π_z orbital. In the basis of the atomic orbitals, the tight-binding Hamiltonian H is given by

$$\begin{pmatrix} \epsilon_1 & t(1+\exp^{-ik_y a}) \\ t(1+\exp^{ik_y a}) & \epsilon_1 + D \end{pmatrix}. \tag{1}$$

The low dimensionality of this model can be justified by thinking that the surface states present within the gap have a very small dispersion in the direction JK perpendicular to the chain (see Fig. 2), in comparison with the direction ΓJ parallel to it. This means that the wave functions are well localized along the chains and the interchain interaction is very weak. t is the overlap matrix element while D is the parameter used to describe the opening of the gap.[36] Here we use it to describe the self-consistent QP bands[12] with an opened gap. We have to mention that such a parameter can also be used to describe the effects of symmetry breaks (such as a buckling of the chains) in the ground state.[36] However this is not our case, as the opening of the gap in the GW calculations is due to many-body effects and not to geometric distortions.

The IBZ of the model is a line going from $k_y=0$ to $k_y=\pi/a$.[37] Hence we must map the (two-dimensional) surface band structure into the model's one-dimensional band structure. In our 4×64 sampling of the IBZ (see Fig. 1), for each fixed k_x, we have a line of k points parallel to the y axis. For every k-point line we can diagonalize the Hamiltonian (1), obtaining the two one-dimensional energy bands:

$$E_1(k_y) = \epsilon_1 + \frac{D - \sqrt{D^2 + 16t^2\cos^2(k_y a/2)}}{2}, \tag{2}$$

$$E_2(k_y) = \epsilon_1 + \frac{D + \sqrt{D^2 + 16t^2\cos^2(k_y a/2)}}{2}. \tag{3}$$

Hence, for each fixed k_x, D is equal to the minimum gap at $k_y=\pi/a$, i.e., at a k point lying on the JK line. At the same time, for a generic k_y, its square is given by $E_g^2(k_y)=D^2+16t^2\cos^2(k_y a/2)$. The eigenfunctions of the Hamiltonian (1) are linear combinations of the two atomic orbitals, e.g., $\Psi_j(k_y)=c_{j1}(k_y)\phi_1+c_{j2}(k_y)\phi_2$ $(j=1,2)$, with:

$$\begin{cases} c_{j1}(k_y) = \frac{H_{12}(k_y)}{\sqrt{[E_j(k_y)-\epsilon_1]^2+(H_{12})^2}}, \\ c_{j2}(k_y) = \frac{E_j(k_y)-\epsilon_1}{\sqrt{[E_j(k_y)-\epsilon_1]^2+(H_{12})^2}}. \end{cases} \tag{4}$$

When $k_y=\pi/a$, i.e., along the JK line, where the coupling of the two dangling bonds vanishes, $H_{12}(k_y)=0$, one has for $D>0$

$$c_{11} = -i,$$

$$c_{12} = 0. \tag{5}$$

This means that along the JK line the valence-band wave function is completely localized on atom 1 of the chain, with the dangling bond of the lower energy. Vice versa, it can easily be found that the conduction-band wave function is localized on atom 2.

When the Brillouin zone (BZ) point is far enough from the JK line, so that $16t^2\cos^2(k_y a/2)\gg D^2$, then

$$c_{11}(k_y) = \frac{\exp^{-ik_y a/2}}{\sqrt{2}},$$

$$c_{12}(k_y) = -\frac{1}{\sqrt{2}}. \tag{6}$$

In this BZ region, where the gap $E_g(k_y)$ is much larger than the minimum gap D, the valence wave functions exhibit a delocalized character having exactly the same weight on the two dangling bonds. The same can be stated for the conduction-band wave functions. In between this two limits there will be a region of the BZ where the wave functions will still have most of their weight on one of the two orbitals.

To summarize we can distinguish three regions in the IBZ, namely: (1) $k_y=\pi/a$ (along JK). Here the valence or conduction QP wave functions are localized on one or the other dangling bond of the surface unit cell, respectively. (2) in $D^2>16t^2\cos^2(k_y a/2)$. Here the QP wave functions have still most of the weight on one of the two dangling bonds. (3) in $16t^2\cos^2(k_y a/2)\gg D$. Here the QP wave functions have the weight equally distributed among the two dangling bonds.

Of course the transition between regions 2 and 3 must be smooth. However, the fact that the QP minimum gap is much larger than the DFT one (as proven in Ref. 12) implies that region 2 is much more extended in the QP case than in the DFT case. In this exceeding area of the IBZ, the QP and the DFT wave functions are qualitatively different. In the first case, they are localized on one out of two atoms of the chain; in the latter (which may be simulated by $D\to 0$) they have a delocalized character.

The region of the IBZ where this mainly happens is close to the JK line (the red-shaded area of Fig. 1). This is the very region that gives the strongest contributions to the low-energy optical-absorption peak. In this important part of the IBZ, the KS wave functions are a rather bad zeroth-order approximations of the QP wave functions.

If now we get the expression of the atomic orbital wave functions in terms of the KS ones, we can use it to obtain the QP wave functions using in Eq. (4) the QP parameters. In order to do this, we fit the model's bands with both the DFT and GW surface bands for every k-point line. In this way we obtain a set of four $t^{\mathrm{QP}}(k_x)$ $[t^{\mathrm{DFT}}(k_x)]$ and four $D^{\mathrm{QP}}(k_x)$ $[D^{\mathrm{DFT}}(k_x)]$, and, of course, the expression of the DFT and QP wave functions in terms of the atomic orbitals for each k point. The best-fit parameters are shown in Table I. We note that, since the dispersion along k_x is very weak, the parameters for the different k-point lines are similar, $D_{\mathrm{QP}}=1.1$ eV ($D_{\mathrm{DFT}}\sim 0.1$ eV) and $t_{\mathrm{QP}}\sim 3.2$ eV ($t_{\mathrm{DFT}}\sim 2.2$ eV). We can now invert the expression of the KS wave functions

TABLE I. The best-fit parameters of the Hamiltonian for the four k-point lines in Fig. 1(b). All the parameters are in eV.

k-point line	1	2	3	4
t_{QP}	3.3	3.2	3.1	3.0
t_{DFT}	2.2	2.2	2.1	2.0
D_{QP}	1.1	1.1	1.1	1.1
D_{DFT}	0.1	0.04	0.06	0.09

in terms of the atomic orbitals and determine the QP wave functions.

In Fig. 3, we plot the square modulus of the KS and QP surface-state wave functions of a generic k point belonging to the red-shaded area of Fig. 1(b). As we can see, both the valence and conduction KS states are delocalized while the QP states are localized on one out of every two atoms. The difference between the two kinds of wave functions is not only quantitative but really qualitative.

III. OPTICAL PROPERTIES

In this paragraph we will see how the localization of the chain wave functions is reflected on the optical properties of the system. Of course, within a simplified tight-binding description, we aim at obtaining simply a qualitative insight. This insight, however, is important in understanding the importance of the wave function change on the optical properties of the system. We have calculated the RA spectra at the DFT-RPA (i.e., independent-particle) level, and then including the excitonic effects in the Bethe-Salpeter equation (BSE) framework i.e., for a Coulomb-correlated quasielectron-quasihole pair (for a review see Ref. 38). RAS is a typical optical probe for surfaces.[14] It measures the difference in reflectance Δr between two orthogonal directions in the surface plane (xy), normalized to the mean reflectance. Since in cubic materials, neglecting nonlinear effects, the isotropic contribution from the bulk cancels out, RAS is a surface sensitive technique. It has been shown that,[39–41] within a perturbative scheme with respect to the abrupt Fresnel interface picture, and in the repeated slab framework, the RAS signal can be calculated by

$$\mathrm{Re}\frac{\Delta r}{r} = \frac{4\pi\omega}{c}\mathrm{Im}\frac{\epsilon^{hs}_{yy}(\omega) - \epsilon^{hs}_{xx}(\omega)}{\epsilon_b - 1}, \tag{7}$$

where ϵ^{hs}_{ii} is the so-called half-slab polarizability.[41] As already mentioned, we computed ϵ^{hs}_{ii} at the DFT-RPA and BSE levels.

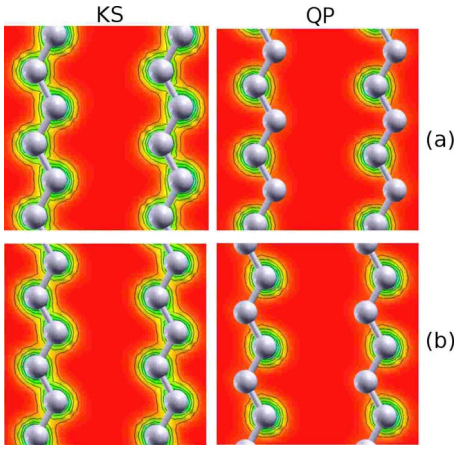

FIG. 3. (Color online) Square modulus of the KS (left) and QP (right) (a) valence and (b) conduction wave functions for a generic point of the red-shaded area of Fig. 1(b). The KS wave functions are delocalized on both atoms of the chain while the QP wave functions are centered on one out of two chain atoms.

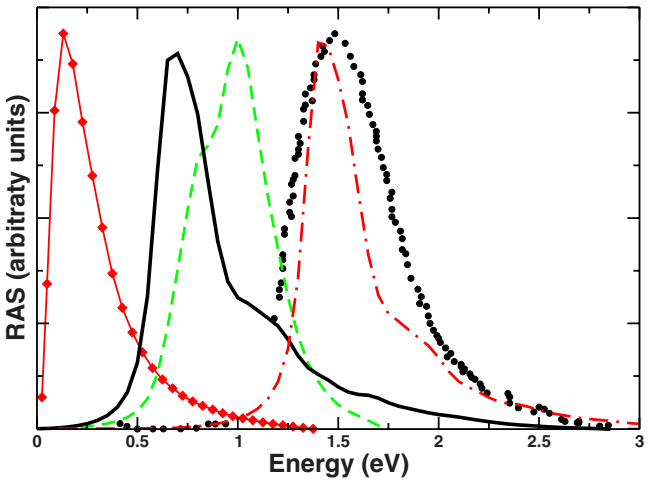

FIG. 4. (Color online) RA spectra calculated at the BSE level employing QP wave functions (full black line for $D=1.1$ eV, and red dot-dashed line for $D=1.8$ eV), employing KS wave functions (green-dashed line), and at the DFT-RPA level (red full line with diamonds). The experimental points from Ref. 15 are shown as black dots. (Surface chains are along the y direction.)

In Fig. 4, we show the calculated RA (Ref. 42) within three approximations. In addition to the mentioned ones, we also plot the result computed using KS wave functions but taken the electron-hole interaction into account (i.e., the standard BSE calculations). The positive peak, also present in a previous tight-binding calculations by Noguez and Ulloa,[43] is due to transitions between surface states. The BSE spectrum computed with the QP wave functions shows a strong RA peak at higher energy with respect to the DFT-RPA one. The corresponding shift in energy can be roughly explained as the sum of a blueshift due to the GW widening of single-(quasi)particle transition energies and a redshift due to the excitonic electron-hole attraction taken into account through the BSE kernel. The difference between the GW gap and the first optic peak gives the theoretical estimation of the exciton binding energy which in this case amounts to 0.4 eV. Its order of magnitude is in agreement with the one of the C(100) surface,[16] where a binding energy of 0.9 eV was found. The reason for a smaller binding energy can be found by comparing the dispersion of the surface bands of the two surfaces. In the case of C(100) the valence and conduction surface bands run parallel to each other all along the Brillouin zone while for C(111) this happens only along JK. The

bound exciton at the C(111)2×1 surface should be hence less localized with a larger average electron-hole distance.

If we compare the computed spectra with the experimental one,[15] we can see that the line shape and the peak is well reproduced. However, although BSE results represent an improvement with respect to DFT-RPA ones, the peak energy (found in the experiment at 1.5 eV) is significantly underestimated. This might be due to the starting point of the optical calculation, namely the *GW* band structure, computed using the KS wave functions in the expression of the self-energy[12] rather than the QP self-consistent wave functions.

The BSE spectra calculated using the KS wave functions (dashed line in Fig. 4) is slightly blueshifted with respect to the BSE spectra computed employing the tight-binding QP ones (full black line). The larger binding energy of the latter can be explained, taking into account the greater semiconducting character of the QP system with respect to the semimetallicity of the KS one. Indeed the semimetallic character of the KS system may give rise to a much more efficient screening of the electron-hole interaction and hence lower the excitonic binding energy.

Even if the peak position is somewhat in better agreement with the experiment in the case of the BSE spectra computed employing the KS wave functions, the line shape of the excitonic spectra is improved using the QP ones. Indeed fitting the tight-binding bands with a larger *ad hoc D* (red dot-dashed line in Fig. 4) returns essentially the experimental spectrum. We would like to emphasize that such a larger *D*, which corresponds to a gap between surface states of about 1.8 eV, is just a fitting parameter.

IV. CONCLUSIONS

In conclusion, we have shown that, through a simple tight-binding model, in the case of the C(111) the surface QP wave functions strongly differ with respect to the KS ones. This happens in a region of the IBZ, close to the *JK* line at the boundary, which is very relevant for the low-energy pair excitations that probe the electronic gap of the surface. Even though it did not solve the disagreement concerning the peak position, the QP wave functions in the excitonic calculations improve the line shape of the spectra compared with the experimental data.

ACKNOWLEDGMENTS

We are grateful for discussions with G. Onida. This work has been supported by the EU through the Nanoquanta Network of Excellence (Contract No. NMP4-CT-2004-500198). Computer resources from INFM "Progetto Calcolo Parallelo" at CINECA are gratefully acknowledged.

[1] J. Isberg, J. Hammersberg, E. Johansson, T. Wikström, D. J. Twitchen, A. J. Whitehead, S. E. Coe, and G. A. Scarsbrook, Science **297**, 1670 (2002).
[2] H. Huang, E. Pierstorff, E. Osawa, and D. Ho, Nano Lett. **7**, 3305 (2007).
[3] N. Tokuda, H. Umezawa, S. G. Ri, M. Ogura, K. Yamabe, H. Okushi, and S. Yamasaki, Diamond Relat. Mater. **17**, 1051 (2008).
[4] J. Ristein, Appl. Phys. A: Mater. Sci. Process. **82**, 377 (2006).
[5] R. Locher, J. Wagner, F. Fuchs, M. Maier, P. Gonon, and P. Koidl, Diamond Relat. Mater. **4**, 678 (1995).
[6] Y. Takano, T. Takenouchi, S. Ishii, S. Ueda, T. Okutsu, I. Sakaguchi, H. Umezawa, H. Kawarada, and M. Tachiki, Diamond Relat. Mater. **16**, 911 (2007).
[7] K. C. Pandey, Phys. Rev. B **25**, 4338 (1982).
[8] F. Bechstedt, A. A. Stekolnikov, J. Furthmüller, and P. Käckell, Phys. Rev. Lett. **87**, 016103 (2001); A. A. Stekolnikov, J. Furthmuller, and F. Bechstedt, Phys. Rev. B **65**, 115318 (2002); D. Vanderbilt and S. G. Louie, *ibid.* **30**, 6118 (1984); A. Scholze, W. G. Schmidt, and F. Bechstedt, *ibid.* **53**, 13725 (1996); G. Kern, J. Hafner, J. Furthmüller, and G. Kresse, Surf. Sci. **357-358**, 422 (1996).
[9] R. Graupner, M. Hollering, A. Ziegler, J. Ristein, L. Ley, and A. Stampfl, Phys. Rev. B **55**, 10841 (1997).
[10] P. Hohenberg and W. Kohn, Phys. Rev. **136**, B864 (1964); W. Kohn and L. J. Sham, *ibid.* **140**, A1133 (1965).
[11] L. Hedin and S. Lundqvist, in *Solid State Physics*, edited by H. Ehrenreich, F. Seitz, and D. Turnbull (Academic, New York, 1969), Vol. 23, p. 1; M. S. Hybertsen and S. G. Louie, Phys. Rev. B **34**, 5390 (1986); R. W. Godby, M. Schlüter, and L. J. Sham, *ibid.* **37**, 10159 (1988).
[12] M. Marsili, O. Pulci, F. Bechstedt, and R. Del Sole, Phys. Rev. B **72**, 115415 (2005).
[13] S. Pepper, Surf. Sci. **123**, 47 (1982).
[14] P. Weightman, D. S. Martin, R. J. Cole, and T. Farrell, Rep. Prog. Phys. **68**, 1251 (2005).
[15] G. Bussetti, C. Goletti, P. Chiaradia, and T. Derry, Europhys. Lett. **79**, 57002 (2007).
[16] M. Palummo, O. Pulci, R. Del Sole, A. Marini, M. Schwitters, S. R. Haines, K. H. Williams, D. S. Martin, P. Weightman, and J. E. Butler, Phys. Rev. Lett. **94**, 087404 (2005).
[17] C. Kress, M. Fiedler, W. G. Schmidt, and F. Bechstedt, Surf. Sci. **331-333**, 1152 (1995).
[18] C. Kress, M. Fielder, and F. Bechstedt, Europhys. Lett. **28**, 433 (1994).
[19] W. J. Huisman, M. Lohmeier, H. A. van der Vegt, J. F. Peters, S. A. de Vries, E. Vlieg, V. H. Etgens, T. E. Derry, and J. F. van der Veen, Surf. Sci. **396**, 241 (1998).
[20] R. P. Chin, J. Y. Huang, Y. R. Shen, T. J. Chuang, and H. Seki, Phys. Rev. B **52**, 5985 (1995).
[21] M. Marsili, O. Pulci, F. Fuchs, F. Bechstedt, and R. Del Sole, Surf. Sci. **601**, 4097 (2007).
[22] S. Walter, J. Bernhardt, U. Starke, K. Heinz, F. Maier, J. Ristein, and L. Ley, J. Phys.: Condens. Matter **14**, 3085 (2002).
[23] O. Pulci, M. Marsili, P. Gori, M. Palummo, A. Cricenti, F. Bechstedt, and R. Del Sole, Appl. Phys. A: Mater. Sci. Process. **85**, 361 (2006).
[24] F. Aryasetiawan and O. Gunnarsson, Rep. Prog. Phys. **61**, 237

(1998).
[25] T. Kotani, M. van Schilfgaarde, and S. V. Faleev, Phys. Rev. B **76**, 165106 (2007).
[26] M. Lopez del Puerto, M. L. Tiago, and J. R. Chelikowsky, Phys. Rev. B **77**, 045404 (2008).
[27] O. Pulci, F. Bechstedt, G. Onida, R. Del Sole, and L. Reining, Phys. Rev. B **60**, 16758 (1999); O. Pulci, L. Reining, G. Onida, R. Del Sole, and F. Bechstedt, Comput. Mater. Sci. **20**, 300 (2001).
[28] J. C. Grossman, M. Rohlfing, L. Mitas, S. G. Louie, and M. L. Cohen, Phys. Rev. Lett. **86**, 472 (2001).
[29] J. L. Li, G. M. Rignanese, E. K. Chang, X. Blase, and S. G. Louie, Phys. Rev. B **66**, 035102 (2002).
[30] F. Fuchs, J. Furthmüller, F. Bechstedt, M. Shishkin, and G. Kresse, Phys. Rev. B **76**, 115109 (2007).
[31] F. Bruneval, N. Vast, L. Reining, M. Izquierdo, F. Sirotti, and N. Barrett, Phys. Rev. Lett. **97**, 267601 (2006).
[32] Fabien Bruneval, Nathalie Vast, and Lucia Reining, Phys. Rev. B **74**, 045102 (2006).
[33] F. Bruneval, F. Sottile, V. Olevano, R. Del Sole, and L. Reining, Phys. Rev. Lett. **94**, 186402 (2005).
[34] M. Gatti, F. Bruneval, V. Olevano, and L. Reining, Phys. Rev. Lett. **99**, 266402 (2007).
[35] F. J. Himpsel, D. E. Eastman, P. Heimann, and J. F. van der Veen, Phys. Rev. B **24**, 7270 (1981).
[36] F. Bechstedt, *Principles of Surface Physics* (Springer, New York, 2003).
[37] The model bands actually fit well to the surface ones only close to the *JK* line while it is much less compatible to the real DFT and *GW* dispersion away from it. As a matter of fact, we need to correct the wave functions only for the k points close to the *JK* line and we will fit the band structure only in a region close to it, namely the red-shaded area in Fig. 1(b).
[38] G. Onida, L. Reining, and A. Rubio, Rev. Mod. Phys. **74**, 601 (2002).
[39] A. Bagchi, R. G. Barrera, and A. K. Rajagopal, Phys. Rev. B **20**, 4824 (1979).
[40] R. Del Sole, Solid State Commun. **37**, 537 (1981).
[41] F. Manghi, R. Del Sole, A. Selloni, and E. Molinari, Phys. Rev. B **41**, 9935 (1990).
[42] In the excitonic calculation we have computed a 1003 $\times$ 1003-G dielectric matrix on an approximate grid made of 51 q points in the IBZ, using 600 empty states and updated energies. The values of the dielectric matrix for the exact 325 q-point grid were then interpolated. Only the resonant part of the excitonic Hamiltonian has been taken into account during the calculation.
[43] C. Noguez and S. E. Ulloa, Phys. Rev. B **53**, 13138 (1996).